

**SYNTHESIS AND ANALYSIS OF  
METHYLAMMONIUM LEAD IODIDE SINGLE  
CRYSTAL PEROVSKITE USING INVERSE  
TEMPERATURE CRYSTALLIZATION METHOD**

**MASTER OF SCIENCE IN PHYSICS**

**2020 – 2022**

# ABSTRACT

Perovskite crystals have received extensive interest in current years because of their facile synthesis and wonderful optoelectronic which includes the long carrier diffusion length, high carrier mobility, low trap density, and tunable absorption edge ranging from ultra-violet (UV) to near infrared (NIR), which give ability for applications in sun cells, photodetectors (PDs), lasers, etc. Here we are going to discuss the synthesis, properties, and applications of Methylammonium lead iodide perovskite single crystals, particularly through the Inverse Temperature Crystallization method. Methylammonium lead iodide perovskite has been of great concern in recent fields of study. They have a direct band gap of 1.6 eV that suits it as a better option for optoelectronic applications. The absorption range of the  $\text{MAPbI}_3$  is very broad. The typical range is from 300 to 800 nm. Longer carrier lifetime and diffusion length of  $\text{MAPbI}_3$  perovskite makes it an essential one in modern technologies. Challenges towards the crystal growth and stability with future scope for study were also briefly described later.

## LIST OF FIGURES

| Figure No   | Name of Figures  | Page No |
|-------------|--|---------|
| Figure 1.1  | Ideal Perovskite Structure                                 | 1       |
| Figure 1.2  | Perovskite Crystal   | 2       |
| Figure 1.3  | Lev Perovski   | 3       |
| Figure 1.4  | Single Perovskite  | 6       |
| Figure 1.5  | Double Perovskite  | 6       |
| Figure 1.6  | Layered Perovskite   | 7       |
| Figure 1.7  | Inverse Temperature Crystallization Method                 | 10      |
| Figure 1.8  | Top Seeded-Solution Growth Method                          | 11      |
| Figure 1.9  | Anti – Solvent Vapour Assisted Crystallization method      | 11      |
| Figure 1.10 | Facile Solution Process Method                             | 12      |
| Figure 1.11 | Optical Images of Laser based MAPbI <sub>3</sub> nanoplate | 13      |
| Figure 1.12 | LED based on Perovskite Single Crystal                     | 13      |
| Figure 1.13 | Photodetector based on Single Crystal Perovskite           | 14      |
| Figure 1.14 | Perovskite Solar Cell                                      | 14      |
| Figure 1.15 | Schematic of SOFC Operating on H <sub>2</sub> or CO        | 15      |
| Figure 2.1  | Lead (II) iodide   | 18      |
| Figure 2.2  | MAI Chemical structure                                     | 19      |
| Figure 2.3  | Methylamine iodide Precursor Salt                          | 19      |
| Figure 2.4  | Growth of Single Crystal in oil bath                       | 21      |
| Figure 2.5  | MAPbI <sub>3</sub> Single Crystal                          | 21      |
| Figure 2.6  | Methylammonium lead iodide Perovskite                      | 22      |
| Figure 2.7  | Bragg Diffraction in a crystal                             | 24      |

|             |   |    |
|-------------|---|----|
| Figure 2.8  | Powder XRD  | 25 |
| Figure 2.9  | Powder XRD Instrumentation set up                             | 26 |
| Figure 2.10 | UV Visible Spectroscopy Principle                             | 27 |
| Figure 2.11 | Schematic representation of dual beam UV Visible Spectroscopy | 28 |
| Figure 2.12 | TGA Equipment   | 29 |
| Figure 2.13 | Schematic Representation of TGA Equipment                     | 29 |
| Figure 2.14 | DSC Equipment   | 31 |
| Figure 2.15 | Schematic Representation of DSC Equipment                     | 32 |
| Figure 2.16 | Heat Flux type DSC  | 33 |
| Figure 2.17 | Power Compensating DSC  | 33 |
| Figure 3.1  | Powder XRD of MAPbI <sub>3</sub>                              | 35 |
| Figure 3.2  | UV Visible Spectroscopy of MAPbI <sub>3</sub>                 | 36 |
| Figure 3.3  | Band gap of MAPbI <sub>3</sub>                                | 37 |
| Figure 3.4  | Thermogravimetric Analysis of MAPbI <sub>3</sub>              | 38 |
| Figure 3.5  | Differential Scanning Calorimetry of MAPbI <sub>3</sub>       | 39 |

# CONTENTS

|   | PAGE NO |
|---|---------|
| ABSTACT   |         |
| LIST OF FIGURES   |         |
| CHAPTER 1 - INTRODUCTION AND OBJECTIVES                   | 1       |
| 1.1 – INTRODUCTION  | 1       |
| 1.2 -HISTORICAL ASPECTS OF PEROVSKITES                    | 3       |
| 1.3 -CLASSIFICATION OF PEROVSKITES                        | 4       |
| 1.4 -PROPERTIES OF PROVSKITES                             | 7       |
| 1.5 -SYNTESIS OF PEROVSKITE                               | 10      |
| 1.6 -APPLICATIONS OF PEROVSKITES                          | 12      |
| 1.7 REVIWEW OF LITERATURE                                 | 15      |
| CHAPTER 2 – MATERIALS AND METHODS                         | 17      |
| 2.1 – SYNTHESIS OF MAPbI <sub>3</sub>                     | 17      |
| 2.1.1 -PRECURSOR SALT                                     | 17      |
| 2.1.1.1 – LEAD(II) IODIDE                                 | 18      |
| 2.1.1.1.1 – SYNTHESIS OF PbI <sub>2</sub>                 | 18      |
| 2.1.1.2 – METHYLAMINE IODIDE                              | 18      |
| 2.1.1.2.1 – SYNTHESIS OF MAI                              | 19      |
| 2.1.2 - PREPERATION OF PRECURSOR SOLUTION                 | 20      |
| 2.1.3 – GROWTH OF SINGLE CRYSTAL                          | 20      |
| 2.1.4 – PROPERTIES OF MAPbI <sub>3</sub> SINGLE CRYSTAL   | 21      |
| 2.1.5 – APPLICATIONS OF MAPbI <sub>3</sub> SINGLE CRYSTAL | 21      |
| 2.1.6 – LIMITATIONS OF MAPbI <sub>3</sub> SINGLE CRYSTAL  | 22      |

|   |    |
|---|----|
| 2.2 – METHYLAMMONIUM LEAD IODIDE PEROVSKITE | 22 |
| 2.3 - CHARACTERISATION TECHNIQUE            | 22 |
| 2.3.1 X RAY DIFFRACTION                     | 23 |
| 2.3.1.1 XRD PRINCIPLE                       | 23 |
| 2.3.1.2 POWDER XRD                          | 24 |
| 2.3.1.3 INSTRUMENTATION                     | 25 |
| 2.3.2 UV VISIBLE SPECTROSCOPY               | 26 |
| 2.3.2.1 INSTRUMENTATION                     | 28 |
| 2.3.3 THERMOGRAVIMETRIC ANALYSIS            | 28 |
| 2.3.3.1 INSTRUMENTATION                     | 30 |
| 2.3.3.2 APPLICATIONS                        | 31 |
| 2.3.4 DIFFERENTIAL SCANNING CALORIMETRY     | 31 |
| 2.3.4.1 INSTRUMENTATION                     | 32 |
| 2.3.4.2 APPLICATIONS                        | 33 |
| CHAPTER 3 - RESULTS AND DISCUSSION          | 34 |
| 3.1 EXPERIMENTAL DETAILS                    | 34 |
| 3.2 POWDER XRD ANALYSIS                     | 35 |
| 3.3 UV SPECTRUM ANALYSIS                    | 36 |
| 3.4 THERMOGRAVIMETRIC ANALYSIS              | 38 |
| 3.5 DIFFERENTIAL SCANNING CALORIMETRY       | 39 |
| 3.6 CONCLUSION                              | 40 |
| SCOPE FOR FUTURE STUDIES                    | 40 |
| REFERENCE                                   | 41 |

# CHAPTER 1

## INTRODUCTION AND OBJECTIVES

### 1.1 - INTRODUCTON

Perovskite single crystals are getting higher importance in recent fields of studies due to their easy synthesis and having very good optical properties such as high carrier mobility, low trap density, long carrier diffusion length and having adjustable absorption edge from UV region to near IR region.

Generally, Perovskites are materials having the general formula of the type  $ABX_3$ . Perovskite materials have a crystal structure similar to  $CaTiO_3$ . The “A and B” in the general formula denotes cations differing in size usually A are larger than B atoms and “X” denotes the anion which gets bounded to both. The family of perovskite material includes numerous types of oxide forms, such as transition metal oxides

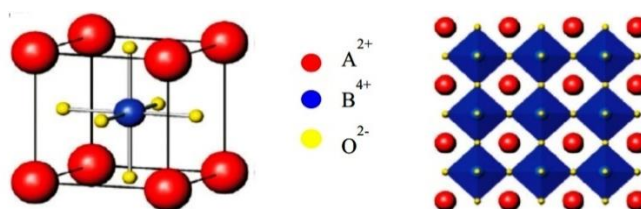


Figure 1.1 Ideal perovskite structure( $ABO_3$ )[1]

Perovskite crystal got its name from calcium titanium oxide and is usually found as yellow, orange, grey, brown or black minerals. Perovskite crystals are cubic or nearly cubic in structure having formula  $ABO_3$ [2]. Perovskite has a highly stable structure. Saying it to be nearly cubic the “A” atoms form the corners of the cubic cells have 12-fold coordination number, “B” atoms in centre forming 6-fold coordination and octahedron of anions in surroundings.

Victor Moritz Goldschmidt discovered an empirical relationship known as tolerance factor ( $t$ ) to estimate the stability of a perovskite structure. This relation is valid for the relevant ionic radii at room temperature. The Goldschmidt tolerance factor can be found out by using the equation

$$t = \frac{RA+RB}{\sqrt{2}(RB+RX)} \quad [3] \quad (1)$$

where  $RA$ ,  $RX$ ,  $RB$  are the ionic radii respectively.

The ratio of ionic radius of  $B$  to ionic radius of  $O$  (generally  $O$  denoted by  $X$ ) is called as “ $\mu$ ”.

$$\mu = \frac{RB}{RX} \quad (2)$$

The perovskite structure is stable when  $0.89 \leq t \leq 1.06$ . Ions are small,  $t < 1$ , and tetragonal, orthorhombic and rhombohedral deformations of structure due to rotation and tilting of the  $BO_6$  octahedral are observed. Only at room temperatures we can obtain cubic structure ideally.



Figure 1.2 - Perovskite Crystal[3]

Perovskite materials show a wide range of properties due to their characteristic chemical nature such as their non-stoichiometry of the anions and/or cations, the valence mixture electronic structure, the distortion of the cation configuration and mixed valence. Halide perovskites are becoming very important materials for optoelectronic devices. These materials have great applications on light emitting diodes (LEDs), photodetectors and lasers as well. Rapid advances in bulk perovskite materials aroused universal interest for



the development of perovskite nanocrystals, Perovskite nanocrystals have exhibited high luminescence quantum yield, sharp emission peak, and emission colour tunability. The progress in these crystals have made them a great application in the lasers and light emitting diodes .

Perovskite crystals for sure an indispensable part of commercial and industrial field applications. Various perovskite crystal can be made by using chemical principles and it will be a boon in future. Perovskite materials can function efficiently both as a film in light-emitting diodes and also in the form of nanoparticles in light-emitting electrochemical cells. Perovskite materials have indeed a very bright future.

## **1.2 HISTORICAL ASPECTS OF PEROVSKITES**



Figure 1.3 - Lev Perovski[4]

Perovskite is a yellow , brown, or black minerals, having a common general formula as  $\text{CaTiO}_3$ . It obtains its name from mineral named as calcium titanium oxide and it was discovered by Gustav Rose in the Ural Mounts of Russia. The name Perovskite came after Lev Perovski (1792–1856) who was the first discoverer in 1792. The material has a cubic structure. The most common perovskite crystals are  $\text{CaTiO}_3$  and  $\text{BaTiO}_3$ .

The mineral was discovered in the Ural Mountains of Russia by Gustav Rose in 1839 and is named after Russian mineralogist Lev Perovski (1792–1856). Perovskite's notable crystal structure was first described by Victor Goldschmidt in 1926 in his work on tolerance factors. The crystal structure was later published in 1945 from X-ray diffraction data on barium titanate by Helen Dick Megaw.

Perovskite would have remained unexplored until if V.M. Goldschmidt, the founder of the science of crystal chemistry and his school of geochemists in Oslo shows no interest in it. Goldschmidt synthesised and studied a large number of the first synthetic Verbindung perovskites with different compositions, including  $\text{BaTiO}_3$ , in 1924-26. "Geochemische Verteilungsgesetze der Elemente" is the classic reference of Goldschmidt in material synthesis.

Goldschmidt started determining the crystal structure of each of the phase of  $\text{ABX}_3$  compounds. This leads to a major development in the crystal Chemistry. He synthesized a large number of isostructural phases. The tolerance factor was also introduced by him.

Helen Dick Megaw worked out the crystal structure of barium titanate, used in capacitors, pressure sensitive devices and other electrical and optical applications. Her studies are very valuable that Megaw's name became associated with perovskite structures. Megawite ( $\text{CaSnO}_3$ ), a perovskite-group mineral, is indeed named after her.

Halide perovskite single crystals have acquired great admire since they can be grown from low-cost solution processes with great potential for future commercialization in optoelectronic devices, [5] especially for radiation detectors. The strong stopping power, absence of deep traps, large mobility ( $\mu$ ) and lifetime ( $\tau$ ), product, and easy crystallization from low-cost solution processes make perovskite single crystals suitable for next-generation ionization detection materials.

Still the applicability is limited for some crystals in the performance side. It has to be improved. Obtaining high-quality perovskite crystal materials is must for better performance and stability. Perovskite crystal with fewer defects is to be made. More studies and works are still needed.

### **1.3 CLASSIFICATION OF PEROVSKITES**

Perovskite material is a material with chemical formula  $\text{ABX}_3$ -type, which exhibits a similar crystal structure of  $\text{CaTiO}_3$ .

It can be generally classified into [6]-

- Inorganic oxide perovskites- These perovskites include intrinsic perovskites and doped perovskites with reference to chemical constituents on their peculiar sites. Frequently the inorganic perovskite oxides changes from the ideal cubic structure rely on the size of A- and B- site cations. [6]Structural changes of those depends on alteration in temperature and pressure and also the properties get changed due to the oxygen vacancies. These are rarely shown by other types. By doping the oxygen vacancies in these can be controlled.
- Hydride perovskite- ABXr type pure hydride perovskites, such as NaMgH, MgXH, (X = Fe, Co), and borohydride perovskites AS(BH<sub>4</sub>)<sub>3</sub> are included in the hydride perovskite type. Hydride perovskites are formed when the stoichiometric ratio of the hydrides of A- and B-site cations are heated (~673 K) under a high-pressure atmosphere. It is a reversible process, and the hydrogen gets got out ~673. Hence, these materials are widely analysed as hydrogen storage materials.
- Perovskite hydroxide- Perovskite hydroxide is those of type having formula AB(OH)<sub>6</sub> with double perovskite structure. Catalytic properties are shown by these materials because of their special optical and electronic properties. Examples of these types include, ASn(OH)<sub>6</sub> (A=Mg, Sr, Ba, Zn, Cu, Co, Fe, Mn, etc.)
- Halide perovskite- These types of perovskites include alkali halide perovskites and organometal halide perovskites. Efforts are made to produce perovskite structured fluorides with the general formula AMF, (where A = Na, K, Cs, Rb, etc., M = Mn, Fe, Co, Ni, Zn, Mg, Cu, etc.). Normally these perovskite fluorides display antiferromagnetic properties, and some are excellent provider for luminescent ion. Perovskite structured halides having general formula ABX, (where A = Cs, B = Pb, Sn, X = Cl, Br, and I) got huge recognition because of their higher-level optical properties. The amenability on the perovskite lattice sites allows the occupancy of inorganic cations such as CH<sub>3</sub>NH<sub>3</sub><sup>+</sup> in the A site resulting in the formation of organic-inorganic hybrid halides such as (CH<sub>3</sub>NH<sub>3</sub>)PbX, (where X = Cl, Br, I or a combination of these anions). The perovskite structured APbX, (A = Cs, CH<sub>3</sub>NH<sub>3</sub><sup>+</sup>, etc.; X = Br, I, etc.) shows excellent characters suitable for optoelectronic applications. Because of the toxicity of Pb and instability in the open air, lead-based halide perovskites

have a limited commercial application. Toxic free , environmentally friendly double perovskite halides which can be tuned are recently available.

In terms of perovskite structures, perovskites can be classified into,

- **Single perovskites** - Single perovskites are those which takes a low symmetrical triclinic to high symmetric cubic phases. These perovskites are studied the most, and their properties can be altered simply by doping.

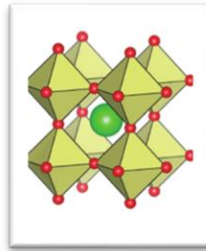


Figure 1.4 - Single perovskite[7]

Single perovskite oxide structures with alkaline earth metal or rare earth metals at the A-site and transition metal at the B-site are analysed the most among single perovskites. Most single perovskites can be synthesized simply at low temperatures using conventional techniques.

- **Double perovskites** - Double perovskites having the formula  $AB_2X_6$  are also made following the advantages of  $ABX_3$  perovskite structured materials. The presence of two property determining B-site cations is likely to exhibit superior properties than  $ABX_3$  perovskite materials, particularly among the halide perovskites for optoelectronic applications.

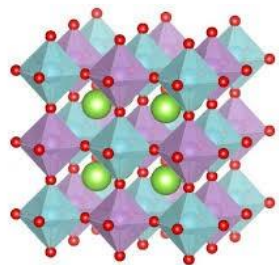


Figure 1.5 - Double perovskite [7]

- **Layered perovskites** - The layered perovskites are further classified into Ruddlesden-Popper phase, the Dion-Jacobson phase, the Aurivillius phase, and  $A_nB_{n-1}O_{3n-1}$  layered phase.

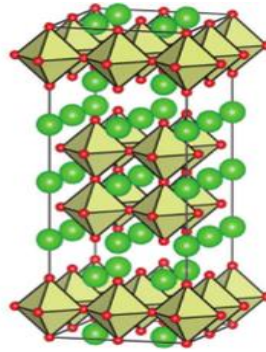


Figure 1.6 - Layered perovskite[7]

These types of perovskites show exceptional peculiarities, such as superconductivity, that are not observed in single or double perovskite crystals. This is due to the oxygen-rich separating layers between the perovskite slabs. In common, the layered perovskites reveal anisotropy in their properties along the *ab*-plane and *c*-axis. This type of perovskite crystal emerged as a solution to the stability related matters.

#### 1.4 - **PROPERTIES OF PEROVSKITE**

Perovskite materials exhibit a wide variety of interesting properties like ferroelectric, dielectric, optical, pyroelectric, and piezoelectric behaviour[6]. Many of the physical properties of perovskite-phase materials are dependent on their phase transitions. It depends on things such as chemical composition, purity, number of surface and bulk defects, grain size, and sintering conditions.

- **Optical properties** - Perovskites give a variety of materials with magnificent optical and photoluminescence characters. The single crystal of BaTiO<sub>3</sub>, 0.25 mm thick transmit from 0.5  $\mu$  to 6  $\mu$ . 0.20  $\mu$  to 17  $\mu$  is the wavelength range in which optical coefficient of strontium titanate crystal.

The optical density of  $\text{CaTiO}_3$  show absorption properties approximately equal as  $\text{SrTiO}_3$  crystals. A few perovskites electro-optic coefficient doesn't change with temperature. Potassium tantalate niobate (KTN) is one of the perovskite oxides having room temperature electro-optic properties and wide-angle fast optical beam scanner. Hence these perovskites are used in optical communications and lasers.  $\text{BaZrO}_3$  emits light in the visible region and available at low cost. It is used in applications such as scintillators, solid state lighting, field emission displays, green photocatalyst and plasma displays.[8]

- **Dielectric Properties** - Layers of dielectric materials are often inserted into capacitors to increase their performance. Electrostatic fields can preserve for a long time in these materials. Several methods have been adopted to explain the dielectric and mechanical properties of these type of materials. Relaxor ferroelectric is one of the routes, which show some effects due to slow reduction processes for temperatures higher to glass transition.[8]
- **Ferroelectricity** - Ferroelectricity is a property that occurs when some material gets external electric field leading to electric polarization. Identifying ferroelectricity in perovskite-based things and other barium titanate ( $\text{BaTiO}_3$ ) reveals a variety of applications for ferroelectric materials. This leads to a subject of study in other types of ferroelectrics.[8] Ferroelectric property is widely used in ultrasound imaging devices, fire sensors, infrared cameras, vibration sensors, tuneable capacitors, memory devices, RAM and RFID cards, input devices in ultrasound imaging, and to make sensors, capacitors etc. A well-known ferroelectric material is  $\text{BaTiO}_3$  with relative dielectric constant. No net polarization is exhibited by its crystal at room temperature and not in the presence of an external field.
- **Piezoelectricity** - Piezoelectricity is the capacity of materials to produce an electric charge in reaction to applied mechanical stress. When mechanical strain is applied to definite crystals, they became polarized at a degree which is proportional to the applied strain.[9] Examples of synthetic piezoelectric materials are the piezoelectric ceramics with the perovskite crystal structure being of the formula  $\text{A}_2\text{B}_4\text{O}_{12}$ . Examples of naturally available piezoelectric materials are quartz, cane sugar, collagen, topaz, Rochelle salt,

tendon, etc. Piezoelectric property is applicable in Cigarette lighter, Sensors, Microphones, High voltage and power source, Pick-ups, Pressure sensor, Force sensor, Strain gauge, Actuators, Piezoelectric motors, Piezoelectric motors, Nano-positioning in AFM, STM etc.

- **Catalytic Activity** - The perovskite structure showed high catalytic activity. Also, their stability made the preparation of several compounds from elements with uncommon valence statuses or a lack in oxygen. They motor exhaust are also seen as gas catalyst, cleaning catalyst, and intelligent automobile catalyst for various catalytic environmental reactions. Some Perovskite types (containing Cu, Co, Mn, or Fe) showed catalytic action to the straight decay of NO at high temperature due to the occurrence of oxygen deficiency. Perovskite got a wide application as a vehicle catalyst, intelligent catalyst, removal of CO & NO, effective catalyst and not combusted hydrocarbons. Because of the great stability of the perovskite structure and the unlimited spreading state of Pd it is commonly called as intelligent catalyst.
- **Superconductivity** - Superconductivity is the phenomenon in which certain materials once cooled under a specific serious temperature exhibit null electrical resistance and magnetic flux gets expelled. The oxide perovskite's structure type provides an excellent structural framework due to the existence of superconductivity. The first discovered example of superconducting perovskites is La-Ba-Cu-O perovskite. Type 2 group Superconducting "perovskites" metal-oxide ceramics are those compounds which have specific ratio of 2 metal atoms to every 3 oxygen atoms. This type of superconductors is made up of alloys and metallic compounds. Nowadays they achieve higher transition temperature than Type 1 superconductors.[9]
- **Colossal Magneto Resistance (CMR)** - It is the property of certain materials that allows them to alter their electrical resistance in the presence of a magnetic field. Magnetic phases can be identified depending on the orbital occupancy of the manganese ions and the associated orbital order. In this type of materials, ordering temperatures of similar magnitude for both degrees of freedom due to their orbitals and spins are coupled very strong. CMR effect is dependent to its manganates which are correlated electron

systems with interplay among the lattice spin, Jahn-Taller effect, charge & orbital degrees of freedom, electronic phase separation, charge ordering, etc.

- **Quantum paraelectrics** - The property of substances to show behaviour that has an impending phase transition at low temperatures. The temperature is enough to activate quantum effects. The effect is observed only in certain materials, e.g.,  $\text{SrTiO}_3$ ,  $\text{KTaO}_3$ ,  $\text{CaTiO}_3$ .

## 1.5 - **SYNTHESIS OF PEROVSKITE**

The most common methods of synthesis of perovskites include the methods of ceramic as well as coprecipitation. It is of great importance to make perovskite crystals in an affordable and easy way. The synthesis methods have been advanced throughout the time, comparatively to that of old times. Earlier methods have many drawbacks because of random heating of metal oxides and salts. New methods have been developed to overcome this.[10]

- **Inverse Temperature Crystallization Method** - In inverse temperature crystallization method the solution is heated at fixed temperatures to grow single crystals in a bottle. The surface of solution is in saturated state and bottom of it will be unsaturated at the initial time. Because of the process of convection taking place inside the bottle, concentration will exceed the solubility of precursors and it leads to growth of single crystal. The formerly developed one is used as the nucleation site for the synthesis of our desired large crystals. If the given temperature is too high, then small crystals will be formed, or we get some defect crystals and also there arises a problem that if the temperature decreases too low to room temperature the crystal gets redissolved. Inverse temperature crystallization method is used mainly in the synthesis of multi-component single crystals.[11]

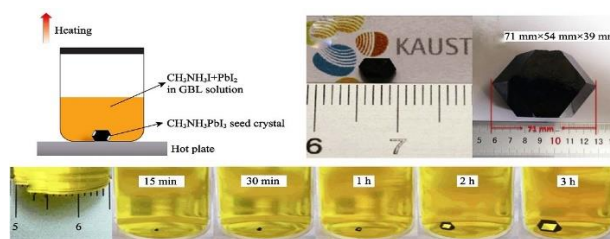


Figure 1.7 - Inverse Temperature Crystallization Method[12]



- **Solution Temperature Lowering (STL) Method** - We have to mention Webber's method that use the difference in solubility of perovskite precursors. The STL method makes use of this method. Primarily the precursors of our perovskites are dissolved into solvents at comparatively higher temperature. Then the temperature is gradually reduced where we would get a stage where the growth of single crystals take place.  
Various methods of Solution Temperature Lowering Method include Bottom-Seeded STL method and Top-Seeded solution growth (TSSG) method.

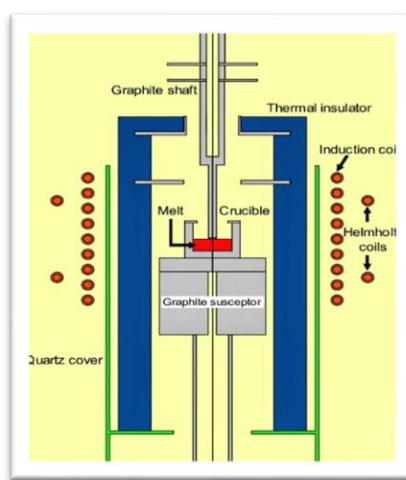


Figure 1.8 - Top-Seeded Solution Growth Method (TSSG)[13]

- **Anti-Solvent Vapour-Assisted Crystallization (AVC) Method** - AVC method is a high-performance room temperature fabrication method for low-cost perovskite crystals. It is an effective method of fabricating single crystals with high quality where the solubility of precursor solution in different solvents are used. Antisolvent crystallization gains supersaturation and solidification by exposing a solution of the material to another one where the product is meagrely soluble.[14] The method is that the precursor of ours is put into the closed bottled containing antisolvent. The solubility of mixed solvent gets reduced when antisolvent diffuses into the precursor solution. Finally, it results in the growth of our desired crystals.

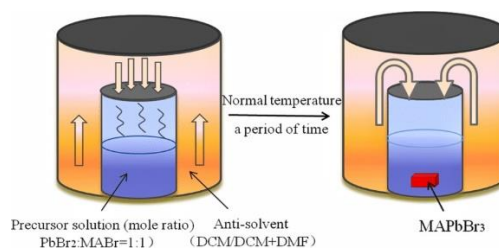


Figure 1.9 – Anti-Solvent Vapour-Assisted Crystallization (AVC) Method[14]

- **Thickness Controllable Methods** - Thickness controllable methods include, Cavitation-Triggered Asymmetrical Crystallization (CTAC) strategy, Facile Solution-Processes Method, Vertical Bridgman Technique, Space-Limited Inverse Temperature Crystallization (SLITC) etc. Controlling the thickness of the crystal is of great importance.

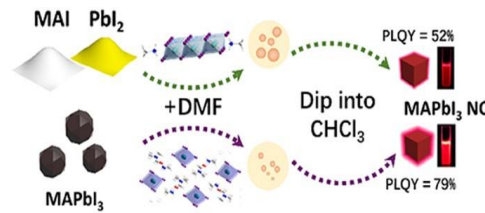


Figure 1.10 - Facile Solution-Process Method

There is a nucleation energy barrier causing the bulk and uneven distribution on our single crystal's surface. It is controlled by ultrasonic pulses which contributes to the cavitation process. The thickness can be controlled within a particular range by shearing force. [9]

## 1.6 - APPLICATIONS OF PEROVSKITES

Perovskites have wide applications in various optoelectronic fields including solar cells, light-emitting diodes, photodetectors, lasers etc. They have very special optical and electronic properties. They are the base of sensors, detectors, CPUs, etc. Hybrid perovskites have greater applications in solar cells, lasers, photodetectors, etc. Single crystals have an upper hand due to their specific features. Grain-boundary-free single-crystal perovskites have the properties of lower trap-state densities, high carrier mobilities, and longer diffusion lengths. Thus, it shows superior optoelectronic performance. Single-crystal thin films gains higher importance for exploring the capabilities of single-crystal perovskites to a great extend in several applications.[8]

- **LASER**- In lasing applications, hybrid perovskites exhibit high optical gains because of low defect density, high absorption coefficient, long carrier diffusion length, high photoluminescence quantum yield, tuneable emission wavelength peaks etc. Lasers fabricated by perovskite single crystals earned

a huge attention because of outstanding performance, including optical-gain media, spectrally narrow gain profiles, high quality factors, and low lasing thresholds. Almost all perovskite lasers use the Whispering-gallery-mode (WGM) cavity.

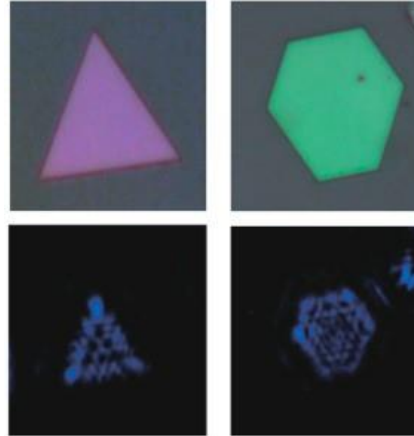


Figure 1.11 - Optical Images of Lasers based on MAPbI<sub>3</sub> nanoplates

- **Light Emitting Diodes (LEDs)** - High-quality perovskite layer is essential for fabricating efficient LEDs because electroluminescence property of perovskite semiconductors can be operated only at liquid nitrogen temperature.[15] Nowadays Perovskite single-crystalline MAPbBr<sub>3</sub> nanoplates are produced by the modified ligand-assisted precipitation method. The outcome showed that enhanced moisture resistance caused by hydrophobicity at the end of the long chains, bringing promise for LED devices.

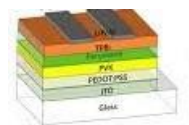


Figure 1.12 – LED Based on Perovskite Single Crystal[15]

- **Photodetectors (PDs)** - Photodetectors can be performed in camera imaging, medical equipment, communication devices etc. PDs based on perovskite single crystals are better in terms of their overall performance and operational stability compared to conventional polycrystalline based PDs. [16]The basic parameters to evaluate PDs are the responsivity (R) and EQE where R describes the response efficiency of optical to electronic signals,

reflecting the efficiency of response to the optical signal.  $R$  is defined as the ratio of photocurrent to incident light intensity.  $\text{MAPbBr}_3$  single crystals show a high product and low surface recombination velocity. This is used in the sensitive X-ray detectors. The sensitivity for X-ray PDs can be achieved as high as  $80 \mu\text{C}\cdot\text{Gy}^{-1}\text{cm}^{-2}$ , which is four times higher than  $\alpha\text{-Se}$  detectors. This discovery leads to a wide range of use of single-crystal PDs in the field of medicine.

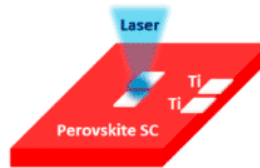


Figure 1.13 - Photodetector based on single crystal perovskite[16]

- Solar Cells** - Solar cells are devices that use the photovoltaic effect that converts the solar energy or the energy from light directly into electrical energy. It produces electrical charges that can move freely in semiconductors. The first solar cell was invented by Bell executives in 1954. As a semiconductor material with a large absorption coefficient and long carrier diffusion length, solar cells should be the best model device to show their advantages, which are similar to a perovskite single crystal. Metal halide single-crystal PSCs are suitable for maximum efficiency and improved stability. The highest efficiency of single crystal-based PSCs has attained 21.09%. Single-crystal perovskites, with their orders of magnitude lower density and higher carrier diffusion length compared with their polycrystalline counterparts, offer a way for the PSC technology to overcome the limitation of polycrystalline thin films and gets close to the Shockley-Queisser limit.

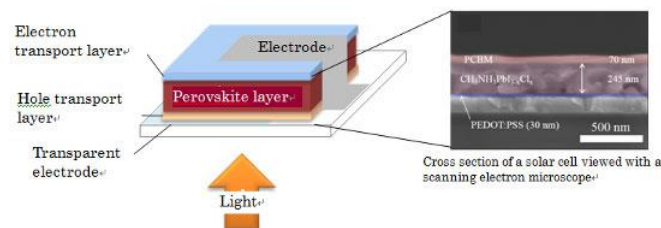


Figure 1.14 - Perovskite Solar Cell

- **Sensors and Biosensors** - Perovskite materials can be used as good sensors of gases like CO, NO<sub>2</sub>, methanol, ethanol etc. It is shown by perovskites having cobaltite, titanates and ferrates. The non-enzymatic glucose sensors that is inorganic perovskite oxides have electrocatalytic activity towards glucose in alkaline medium due to large number of active sites in the modifiers.
- **Solid Oxide Fuel Cells** - A Solid Oxide Fuel Cell (SOFC) is capable of efficiently transforming chemical energy into electrical energy. It can operate on any combustible fuel such as carbon monoxide, hydrocarbons, and coal. SOFCs are based on ceramic membranes that are oxygen-ion conductors. At high temperatures there are challenges for small-scale applications, portable SOFC using as battery replacements and microchip power sources are produced widely. By replacing Ni with Cu or a conducting ceramic, the SOFC can be made to operate with methane and even liquid fuels.

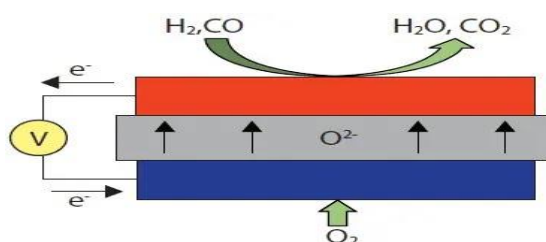


Figure 1.15 - Schematic of SOFC operating on H<sub>2</sub> or CO.

## 1.7- REVIEW OF LITERATURE

**1. Eman Abdul Rahman Assirey** - The perovskite organometallic halide, which demonstrated effective crucial features for photovoltaic solar cells, is examined in this work. The review covers every aspect of perovskites' development, structure, and related applications. Based on A and B site occupancy, the distinctive perovskite structure has the potential to produce a multitude of new compounds, giving rise to a large variety of materials systems with distinct features and several applications. Perovskites compounds were synthesised using a variety of techniques, including co-precipitation, solid-state reactions, hydrothermal synthesis, Pechini, gas phase preparations, sol-gel, low temperature solution combustion, microwave synthesis,

and the use of PVD techniques like laser ablation, MBE, and wet chemical techniques. Materials for numerous commercial and specialised technologies were produced by the variety of perovskite compound synthesis techniques.

**2. Shan-Shan Rong ,M. Bilal Faheem, Yan-Bo Li** – This article discusses the characteristics of perovskite crystals, which have attracted a lot of interest recently due to their simple synthesis and superior optoelectronic properties, such as their long carrier diffusion length, high carrier mobility, low trap density, and tunable absorption edge ranging from ultraviolet (UV) to near-infrared (NIR), which have the potential to be used in solar cells, photodetectors (PDs), lasers, and other devices. Applications of all-inorganic and mixed organic-inorganic perovskite single crystals, as well as their characteristics, are also discussed, with a focus on solution production. At the conclusion of this manuscript, challenges for crystal development and stability about the future were also briefly discussed.

**3. A.S. Bhalla, Ruyan Guo , Rustum Roy** - It is demonstrated that the most adaptable ceramic host is the perovskite structure. The most important electro-ceramic dielectric (BaTiO and its cousins) phase in industry can be converted into metallic conductors, superconductors, or the earth's greatest pressure phases by making the proper compositional adjustments. The most recent research on novel usage in piezoelectric, ferroelectric, and related applications receives extensive discussion after a historical introduction to the science. From the macro to the nanoscale, this article has already found several extremely technologically significant features in this family of materials. The report describes molecules with a perovskite structure as being a crucial component of future strategic and commercially significant technologies.

# CHAPTER 2

## MATERIALS AND METHODS

The materials used , Synthesis methods , Characterisation methods and other sample analysing techniques are studied in this chapter particularly.

### **2.1 - SYNTHESIS OF METHYL AMMONIUM LEAD IODIDE PEROVSKITE (MAPbI<sub>3</sub>) .**

MAPbI<sub>3</sub> was synthesized using Inverse Temperature Crystallization method.[11]

One of the faster methods to grow single crystals of perovskites like MAPbI<sub>3</sub> is Inverse Temperature Crystallization (ITC) method while techniques like Solution Temperature Lowering method (STL) or Anti-solvent Vapour Assisted Crystallization (AVAC) is more time consuming to grow a single crystal of preferred quantity. Inverse Temperature Crystallization method utilises the retrograde solubility of perovskite in specific solvents . The inverse temperature dependence i.e., solubility of a given solute in a given solvent increases with temperature, but some solutes become less soluble as temperature increases is called retrograde or inverse solubility. Therefore, the dissolution of a salt showing retrograde solubility in a given salt is exothermic in nature. The modified ITC approach is very effective in growing large single crystals even at low temperature . We place a seed crystal into the ITC precursor. The method has been altered efficiently by taking the anti-solvent in the precursor, which is either in liquid or vapour form, that has poor solubility with the precursor components and Methylammonium iodide (MAI) [6].

#### **2.1.1 - PRECURSOR SALT**

Two precursor salts are being used for the synthesis of our desired MAPbI<sub>3</sub>, namely

- LEAD (II) IODIDE (PbI<sub>2</sub>)
- METHYLAMINE IODIDE (MAI)

### 2.1.1.1 - LEAD(II) IODIDE (PbI<sub>2</sub>)

Lead iodide is a precursor material in the manufacture of highly efficient solar cells. It consists of many small hexagonal platelets, giving the yellow precipitate a silky appearance. Lead(II) iodide commonly called plumbous iodide having chemical formula PbI<sub>2</sub>. The molar mass of lead(II) iodide is 461.01 g/mol. The compound is colourless when dissolved in hot water. It crystallizes on cooling and visibly larger bright yellow flakes, that settle slowly through the liquid can be seen.

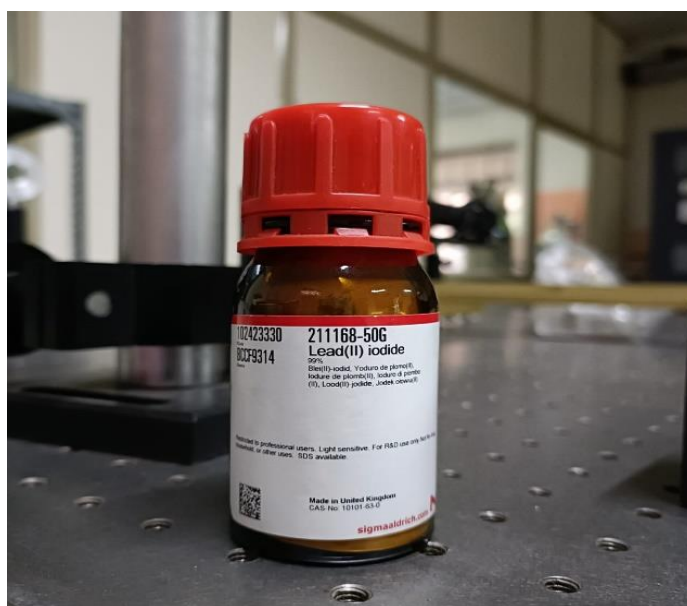


Figure 2.1 - Lead(II) Iodide

#### 2.1.1.1.1 - SYNTHESIS OF LEAD(II) IODIDE

PbI<sub>2</sub> is widely prepared by a precipitation reaction between Potassium Iodide (KI) and Lead(II) Nitrate (Pb(NO<sub>3</sub>)<sub>2</sub>) in water solution:



### 2.1.1.2 - METHYLAMINE IODIDE (MAI)

Methylammonium iodide is an organic halide having formula CH<sub>6</sub>IN. The salt is an ammonium salt which is a composition of methylamine and hydrogen iodide.



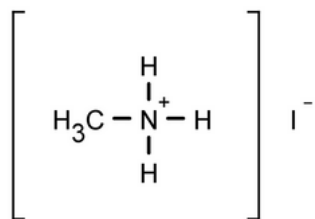


Figure 2.2 - MAI Chemical Structure

The IUPAC name of MAI is known as Methylazanium iodide . Methylammonium iodide (MAI) , also known as methylamine hydroiodide is one of the precursors used in the synthesis of organic-inorganic hybrid perovskites . The hydrogen bonding is there which holds the monomers and dimers. MAI has a molar mass of 158.970 g/mol with topological polar surface area of 27.6 Å². MAI is commonly found in white crystalline form with a purity of 99.9 % as per elemental analysis .

#### **2.1.1.2.1 - SYNTHESIS OF METHYLAMINE IODIDE**

Methylamine Iodide was produced by adding aqueous HI into methylamine under constant magnetic stirring at 0 °C. After stirring of about two hours, the solvent is removed by rotary evaporation . Powder which is orange-yellow coloured is obtained when the above-mentioned solution is evaporated using a rotavapor at 75°C for 3 h. The powder thus obtained is dissolved in Ethanol. It is then recrystallized using diethyl ether and rinsed three times with diethyl ether. MAI thus obtained was dried at 60°C in vacuum overnight. The final product in the form of white methylamine iodide powder was saved at 25°C in a desiccator.



Figure 2.3- Methylamine Iodide Precursor Salt

### **2.1.2 - PREPARATION OF PRECURSOR SOLUTION**

Precursor solutions of different concentrations are produced by blending certain quantity of synthesized MAI and PbI<sub>2</sub> in gamma- Butyrolactone (GBL). Synthesised MAI with molar mass of 158.9695 g/mol and molarity 1.23 M is made up to 5 ml in a beaker. The total mass of methylamine iodide used for the synthesis of precursor solution was 2.8352 g. PbI<sub>2</sub> with a molar mass of 461.01 g/mol is made to desired of 5ml having molarity 1.23 M. The total mass of Lead iodide used for the preparation is 0.9776g.

- Molecular weight of MAI = 158.9695 g/mol

Desired final volume of MAI solution = 5 ml

Molarity = 1.23 M

Mass of Methylamine iodide = 2.8352 g

- Molecular weight of PbI<sub>2</sub> = 461.01 g/mol

Desired final volume of PbI<sub>2</sub> = 5 ml

Molarity = 1.23 M

Mass of Lead iodide = 0.9776 g

### **2.1.3 – GROWTH OF SINGLE CRYSTAL**

The mixture of required quantity of MAI and PbI<sub>3</sub> in GBL solvent was placed at 60°C for overnight about 10 h with constant magnetic stirring in a magnetic stirrer. Then it is placed in an oil bath with temperature measurement facility. Then 5 ml of the solution was maintained at different temperatures from 90°C to 110°C on a hot plate for 48 h for the single crystals to grow in the solution.

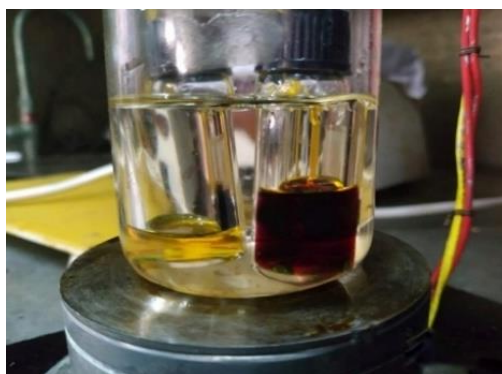


Figure 2.4- Growth of single Crystal in oil bath

To maintain required temperature during crystal growth, silicon oil bath is used for keeping the growth solution. The crystals were taken out from oil bath. It is rinsed with isopropanol and diethyl ether, MAPbI<sub>3</sub> single crystal perovskite is obtained and used for further study.

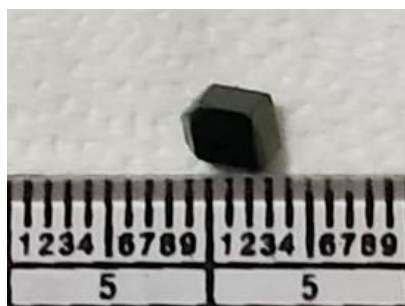


Figure 2.5- MAPbI<sub>3</sub> Single Crystal

#### **2.1.4 - PROPERTIES OF MAPbI<sub>3</sub> SINGLE CRYSTAL PEROVSKITE**

Methylammonium lead iodide perovskite has been of great concern in recent fields of study. They have a direct band gap of 1.6 eV that suits it as a better option for optoelectronic applications. The absorption range of the MAPbI<sub>3</sub> is very broad. The typical range is from 300 to 800 nm. Longer carrier lifetime and diffusion length of MAPbI<sub>3</sub> perovskite makes it an essential one in modern technologies.

#### **2.1.5- APPLICATIONS OF MAPbI<sub>3</sub> SINGLE CRYSTAL PEROVSKITE**

The solar-to-power conversion efficiency of MAPbI<sub>3</sub> is high that makes it suitable for all electronic instruments. MAPbI<sub>3</sub> is a substitute to silicon solar cells which have been developed

based on various dye sensitizers, organic and hybrid (organic inorganic) materials. It has high charge-carrier mobility, which is used for developing high-performance solar cell devices.

### **2.1.6 - LIMITATIONS OF MAPbI<sub>3</sub> SINGLE CRYSTAL PEROVSKITE**

Major drawback is the toxicity of lead which easily degrades on exposure to humidity and ultraviolet (UV) irradiation. Application of Pb-based materials in solar cells is restricted due to their toxicity. Stability is also a major issue. Intrinsic stabilities at the interface and device architecture remain major hindrance for practical applications.

### **2.2 - METHYLAMMONIUM LEAD IODIDE PEROVSKITE**

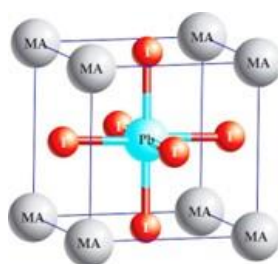
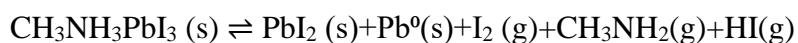


Figure 2.6- Methylammonium Lead Iodide Perovskite[18]

They are in the group of organic - inorganic halide perovskites that exhibit expectational electrical and optical behaviour suitable for photovoltaic applications. At low temperature conditions (< 100 °C) it is found that CH<sub>3</sub>NH<sub>3</sub>PbI<sub>3</sub> undergoes reversible chemical decomposition. I<sub>2</sub> gas is released from MAPbI<sub>3</sub> even in dark conditions during mild heating.



### **2.3 - CHARACTERISATION TECHNIQUES**

Characterization techniques are used to identify crystals, isolate, or quantify materials or to characterize their physical properties, to identify structure, optical, mechanical, electrical, and thermal properties of the grown crystals. They include microscopy, light or radiation scattering, spectroscopy, calorimetry, thermal analysis, chromatography etc. Here we make use of the techniques to characterize the properties of the grown single crystals such structural

(XRD), thermal (TGA/DSC), optical (UV-Visible), vibrational (Raman), hardness and dielectric measurements. In this chapter the discussion will be about structural, optical & thermal analysis techniques used to analyse MAPbI<sub>3</sub> single crystal perovskite.

| Analysis Parameter   | Technique Used  |
|----------------------|---|
| • Structure          | • Powder X-Ray Diffraction  |
| • Optical Properties | • U.V Visible Spectroscopy  |
| • Thermal Properties | • Thermogravimetric Analysis (TGA)<br>• Differential Scanning Calorimetry (DSC) |

### 2.3.1 - X-RAY DIFFRACTION

X-Ray diffraction analysis (XRD) is a commonly used technique that gives detailed information about the crystallographic structure, chemical composition, and physical properties of a material. The technique is based on the constructive interference of monochromatic X-rays and a crystalline sample. X-rays are electromagnetic radiation having shorter wavelength that are produced when electrically charged particles with sufficient energy are decelerated. In XRD, the generated X-rays are collimated and passed to a nanomaterial sample.[19] The interaction of the incident rays with the sample produces a diffracted ray, which is then detected, processed, and counted. The intensity of the diffracted rays scattered at different angles of material are plotted to display a diffraction pattern. Every sample or material produces a unique diffraction pattern. It is useful in many ways like, identifying compounds under investigation, finding lattice strain in case material is deformed, calculating lattice parameter from the peaks, identifying crystal structure and density of compounds.

#### 2.3.1.1 – XRD PRINCIPLE

X-ray diffraction uses the constructive interference of monochromatic X-rays and a crystalline sample. XRD is non-destructive and does not require elaborate sample preparation, which partly explains the wide usage of XRD method in materials characterization diffraction peak

positions are accurately measured with XRD, which makes it the best method for characterizing homogeneous and inhomogeneous strains. X-rays are produced by a cathode ray tube, filtered to produce monochromatic radiation, collimated to concentrate, and directed toward the sample. The interaction of the incident rays with the sample produces constructive interference (and a diffracted ray) when conditions satisfy Bragg's Law  $n\lambda = 2d \sin \theta$  (4). This law relates the wavelength of electromagnetic radiation to the diffraction angle and the lattice spacing in a crystalline sample. These diffracted X-rays are then detected, processed, and counted. By scanning the sample through a range of  $2\theta$  angles, all possible diffraction directions of the lattice should be attained due to the random orientation of the powdered material. Conversion of the diffraction peaks to d-spacings allows identification of the mineral because each mineral has a set of unique d-spacings. Generally, this is achieved by comparison of d-spacings with standard reference patterns.

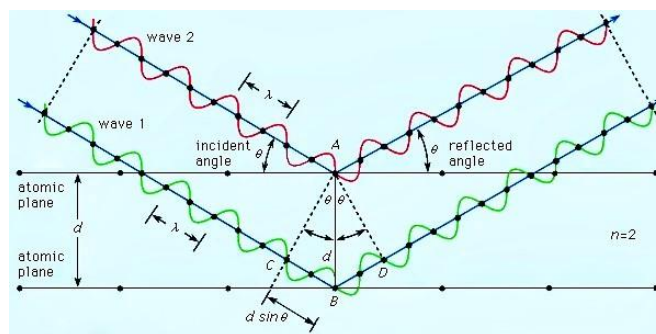


Figure 2.7- Bragg Diffraction in a Crystal

When both crystallite size and inhomogeneous strain contribute to the peak width, these can be separately determined by careful analysis of peak shapes.

### 2.3.1.2 – POWDER X-RAY DIFFRACTION

Powder X-ray diffraction (PXRD) calculates the diffraction pattern of crystalline material. Each will produce a specific pattern according to the structure of its crystal lattice. Each crystalline material will have its own specific pattern. For this reason, PXRD of the API can be done in controlled environmental conditions, using hot stage and/or controlled humidity

environments. In Powder X-ray diffraction, the diffraction pattern is obtained from a powder of the materials not from an individual crystal. Powder X-Ray diffraction is often very easily accessible than single crystal diffraction because it does not require individual crystals. X-ray powder diffraction (XRD) is a rapid analytical technique commonly used for phase identification of a crystalline material [20]. The specimen analysed is finely ground, homogenized. Then the average bulk composition of the compound is determined. Powdered XRD data can look different for particles of the same material that have different morphologies. The peak positions (i.e., x-axis values) will remain the same, but the relative intensities of the peaks (i.e., y-axis values) can change. The particle size of the powder is determined by using the Scherrer formula given by,

$$t = \frac{0.9\lambda}{\sqrt{(BM^2) - BS^2 \cos\theta}} \quad (5)$$

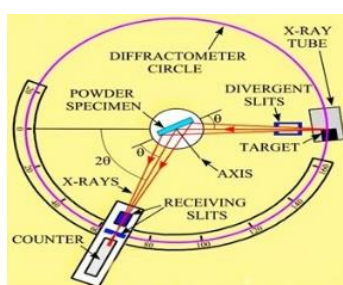


Figure 2.8- Powder XRD

### **2.3.1.3- INSTRUMENTATION**

The XRD analysis of crystalline compounds gives a diffraction pattern consisting of a well-defined, narrow, sharp and significant peak. Many polymers' pictures semi-crystalline behaviour. Powder XRD can be used to determine the crystallinity by comparing the total intensity of the background pattern to that of the sharp peaks. A diffraction pattern plots intensity against the angle of the detector,  $2\theta$ . In a diffraction pattern, the peak position is a variable of wavelength. Absolute intensity (number of X-rays observed in a given peak) might change by instrumental and experimental parameters. Interactions between the incident X-ray beam and the sample produce intense reflected X-rays by constructive interference when conditions satisfy Bragg's Law. The intensity of the reflected X-rays is recorded soon the sample and detector are rotated. The sample rotates in the path of the collimated X-ray beam at an angle  $\theta$ . The X-ray detector is mounted on an arm to collect the diffracted X-rays and

rotates about  $2\theta$ . The instrument used to maintain the angle and rotate the sample is called goniometer. The data is collected at  $2\theta$  from  $\sim 5^\circ$  to  $70^\circ$ , angles. When the geometry of the incident X-rays falling the sample satisfies the Bragg Equation, constructive interference occurs. A peak in intensity occurs. A detector records and processes this X-ray signal and converts the signal to a count rate which is then output to a device such as a printer or computer monitor.

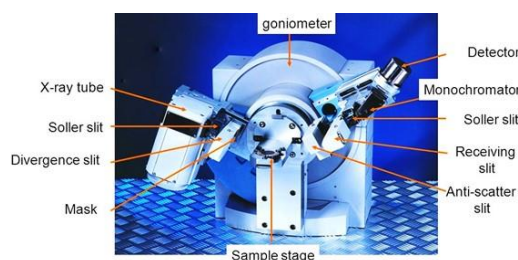


Figure 2.9 - Powder XRD Instrumentation set up[21]

### **2.3.2- UV- VISIBLE SPECTROSCOPY**

UV-Visible spectroscopy is an analytical technique that measures the number/amount of discrete wavelengths of UV or visible light that are absorbed by or transmitted through a sample in comparison to a reference or blank sample. This property is influenced by the sample composition, potentially providing information on what is in the sample and at what concentration.[22]

The absorption of light by any absorbing material is governed by two laws namely,

Bouger -Lambert law and Beer's law. The laws are as follows,

#### **Bouger -Lambert law.**

“The amount of the light absorbed is proportional to the thickness of the absorbing material & is independent of the intensity of the incident light”

$$\ln(I/I_0) = -kb \quad (6)$$

$$\ln(I_0/I) = kb \quad (7)$$

I - Intensity of transmitted light,  $I_0$  - initial intensity of incident light, b-thickness (path - length), k-linear absorption co-efficient



### Beer's law

“The amount of light absorbed by a material is proportional to the number of absorbing molecules 'c' and path length 'b'.

$$A = \epsilon cd \quad [23] \quad (8)$$

$I$  – Intensity of transmitted light,  $I_0$  – initial intensity of incident light,  $\epsilon$  = molar absorptivity,  $d$  = length of light path,  $C$  = concentration.

A distinct spectrum is given by absorbance of radiation by a compound, which helps in identifying the compound. Four possible types of interactions or transitions can be observed. They are ( $\pi-\pi^*$ ,  $n-\pi^*$ ,  $\sigma-\sigma^*$ , and  $n-\sigma^*$ ). The order of the interaction according to the energy is as follows:  $\sigma-\sigma^* > n-\sigma^* > \pi-\pi^* > n-\pi^*$ . The spectrum arises from electron transition in a molecule from a lower level to a higher level.

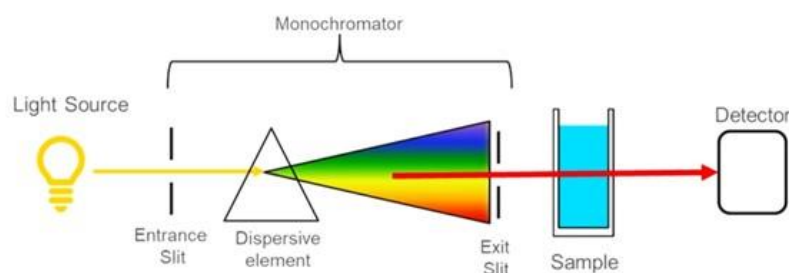


Figure 2.10- UV Visible Spectroscopy Principle[24]

### **2.3.2.1- INSTRUMENTATION OF UV VISIBLE SPECTROSCOPY**

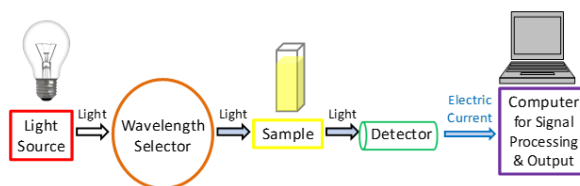


Figure 2.11- Schematic representation of the dual-beam UV-VIS spectrometer

The important parts of the UV Spectrometer include a light source, monochromator, sample holder, Amplifier, detector and recording devices. High-intensity light source is the xenon light source. Standard lamp that emits UV light is deuterium lamp. The light source in the instrument should be changed while our experimental observation. Monochromators changes light into a small band of wavelengths. The wavelength selector that is utilized for the spectrometer light will then pass through the sample. To determine the actual absorbance that the analyser absorb ,the signal from the reference sample can then be used by the instrument . A detector is used to alter the light into a readable electronic signal. A photoelectric coating ejects negatively charged electrons when exposed to light. When electrons are ejected, an electric current proportional to the light intensity is generated. A photomultiplier tube is used in UV-Visible spectroscopy as a detector. When the electric current is generated, the signal is identified and passed to show to a computer or screen.

### **2.3.3 – THERMOGRAVIMETRIC ANALYSIS(TGA)**

Thermogravimetric Analysis is a technique in which the mass of a substance is monitored as a function of temperature or time as the sample specimen is subjected to a controlled temperature program in a controlled atmosphere. A TGA consists of a sample pan that is supported by a precision balance. That pan resides in a furnace and is heated or cooled during the experiment. The mass of the sample is monitored during the experiment. A sample purge gas controls the sample environment. [25]This gas may be inert or a reactive gas that flows over the sample and exits through an exhaust.

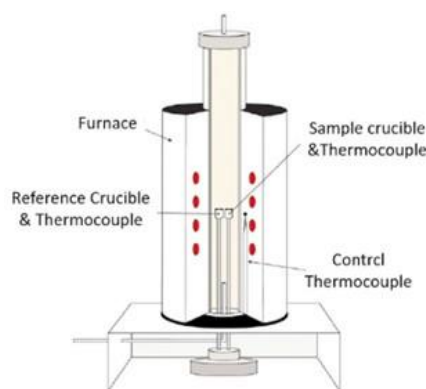


Figure 2.12 – TGA Equipment[26]

In thermogravimetric analysis (TGA), a sample is continually weighted while heating, as an inert gas atmosphere is passed over it. Many solids undergo reactions that evolve gaseous by-products. In TGA, these gaseous by-products are removed and changes in the remaining mass of the sample are recorded. Three variations are commonly employed:

- **Dynamic TGA** - Temperature continues to increase over time as mass is recorded. This allows simultaneous identification of how much gas is removed and the temperature at which it occurs.
- **Static TGA** - Temperature is held constant as the mass is measured. This can be used to gain more information on a decomposition that happens at a certain temperature or to investigate a material's ability to withstand a given temperature.
- **Quasistatic TGA** - Sample is heated in multiple temperature intervals, and held at those intervals for a time, often until the mass stabilizes. This is ideal for investigating substances that are known to decompose in various ways at different temperatures, and better characterizing the way in which they decompose.

In thermo-gravimetric analysis, the sample is heated in each environment (air,  $N_2$ ,  $CO_2$ , He, Ar, etc.) at controlled rate.[26] The change in the weight of the substance is recorded as a function of temperature or time. The temperature is increased at a constant rate for a known initial weight of the substance and the changes in weights are recorded as a function of temperature at different time interval. This plot of weight change against temperature is called thermo-gravimetric curve or thermo-gram, this is the basic principle of TGA.

### 2.3.3.1 – INSTRUMENTATION

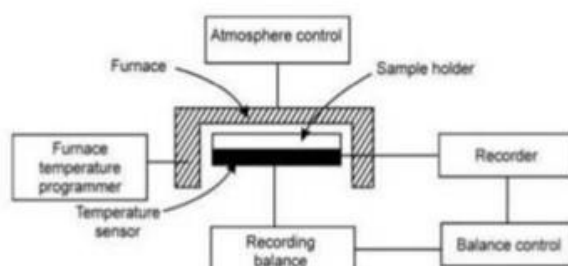


Figure 2.13- Schematic Representation of TGA Instrument

TGA equipment constitutes a highly sensitive balance (a microbalance) for continuous measurement of specimen's weight, a furnace enclosing the sample holder, and a purged gas system to supply gas (inert or reactive, as per the requirement). The furnace is controlled by a computer which also collects the measurement data (sample temperature v/s weight). The balance is calibrated in a manner that a change in weight of the sample produces a proportional electrical signal. A data processing system then collects this electrical signal and converts it into weight or weight loss, which is then plotted on the y axis of the thermal curve. Block diagram of a typical thermogravimetric analysis setup is shown in figure. There are two possible configuration modes of balance and furnace i.e., vertical furnace and horizontal furnace and both suffer from drift with the increase in temperature. Vertical configuration suffers with buoyancy effect attributable to a variation in the density of gas with temperature. Whereas, the horizontal arrangement, which is devised to reduce these buoyancy effects, experiences change in quartz rod length (this rod links the sample to the balance) as the temperature varies. Buoyancy effect is due to the force exerted by fluid that opposes the weight of an increased object modern instruments that heat at rates of 1000 °C/min are available and commercial instruments that heat at rates of 200 °C/min from room temperature to about 1200 °C can also be designed. In these systems, cooling by forced air can be done at 50 °C/min. Sample Preparation maximizing the sample surface area in a TGA pan enhances the resolution and reproducibility of weight loss with temperature. The sample weight influences the accuracy of weight loss measurements. Usually, 10-20 mg of material is desirable in most applications and for volatile materials 20-100 mg of sample is required. The instruments have a baseline drift  $\pm 0.25\%$  of a 10 mg sample.[26]

### **2.3.3.2 – APPLICATIONS**

Thermal stability: Similar or related materials can be contrasted at higher temperatures under desired atmospheric conditions. TGA plot helps to explicate decomposition mechanisms.

Materials Characterization: TGA plot may be employed for material fingerprinting in identification as well as quality control.

Compositional analysis: By a careful choice of temperature programming and gaseous environment, complex materials/mixtures can be examined by removing or decomposing their constituents.

Kinetic studies: Several procedures can help in examining the kinetic features of weight loss or gain through controlling the chemistry or predictive studies.

Corrosion studies: TGA can be used to analyse oxidation or other reactions with different reactive gases or vapours.

### **2.3.4 - DIFFERENTIAL SCANNING CALORIMETRY**

Differential Scanning Calorimetry is the most popular measurement technique to detect endothermic and exothermic transitions like the determination of transformation temperatures and enthalpy of solids and liquids as a function of temperature. Therefore, the sample and reference are maintained at nearly the same temperature throughout the experiment and the heat flux will be measured. DSC enables the measurements of the transition such as the glass transition, melting, and crystallization. [27] Furthermore, the chemical reaction such as thermal curing, heat history, specific heat capacity, and purity analysis are also measurable. Recently, with the development of the highly functional polymeric material, these thermal properties analysis needs are increasing dramatically.



Figure 2.14 – DSC Equipment

As a powerful analytical tool, DSC can elucidate the factors that contribute to the folding and stability of biomolecules. Changes are believed to originate from the disruption of the forces stabilizing native protein structure. For example, this includes van der Waals, hydrophobic, and electrostatic interactions, hydrogen bonds, hydration of the exposed residues, conformational entropy, and the physical environment (such as pH, buffer, ionic strength, excipients). Therefore, thermodynamic parameters obtained from DSC experiments are quite sensitive to the structural state of the biomolecule. Any change in the conformation would affect the position, sharpness, and shape of transition in DSC scans.

#### **2.3.4.1- INSTRUMENTATION**

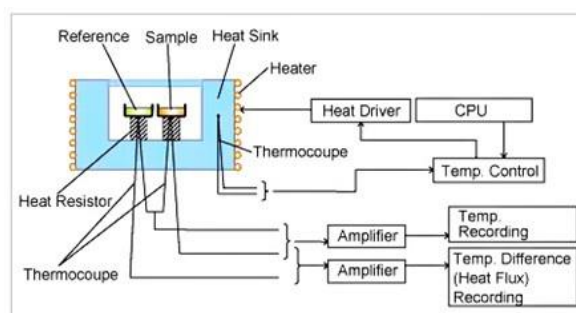


Figure 2.15- Schematic Representation of DSC Equipment[28]

DSC is a commercially available instrument which has two types: Heat Flux Type and Power Compensation Type. Heat Flux DSC comprises the sample and reference holder, the heat resistor, the heat sink, and the heater. Heat of heater is supplied into the sample and the reference through heat sink and heat resistor. Heat flow is proportional to the heat difference of heat sink and holders. Heat sink has the enough heat capacity compared to the sample. In case the sample occurs endothermic or exothermic phenomena such as transition and reaction, this endothermic or exothermic phenomena is compensated by heat sink. Thus, the temperature difference between the sample and the reference is kept constant. The difference the amount of heat supplied to the sample and the reference is proportional to the temperature difference of both holders. By calibrating the standard material, the unknown sample quantitative measurement is achievable.[28]

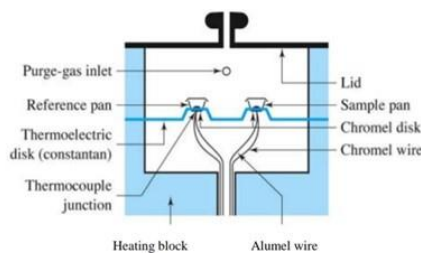


Figure 2.16 – Heat Flux Type DSC

In power differential DSC also known as Power compensating DSC, the sample and reference crucible are placed in thermally insulated furnaces and not next to each other in the same furnace like in Heat-flux-DSC experiments.[29] Then the temperature of both chambers is controlled so that the same temperature is always present on both sides. The electrical power that is required to obtain and maintain this state is then recorded rather than the temperature difference between the two crucibles.

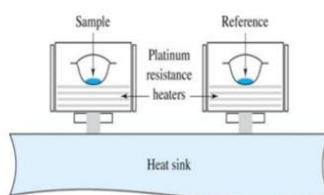


Figure 2.17- Power Compensating DSC[29]

#### 2.3.4.2- APPLICATIONS

DSC analysis is used for numerous applications in a wide range of industries. Examples include glass transition determination and the investigation of chemical reactions, melting and crystallization behaviour. The sensors determine the quality of the measurement and are thus the most important components of the instrument. Better sensitivity means that it is possible to detect smaller thermal effects in the sample or conversely to use smaller amounts of sample. The formation of unique structures of biological macromolecules, such as proteins and their specific complexes, is, in principle, reversible, and the reactions are thermodynamically driven. The direct measurements of the heat effects associated with these intra- and inter macro molecular processes are required by the help of developed, super-sensitive calorimetric techniques such as DSC.[30]

# CHAPTER 3

## RESULTS AND DISCUSSION

Methyl Ammonium Lead Iodide is gaining popularity in research world due to its outstanding optoelectronic properties. Within a time, span of less than a decade perovskite solar cell have achieved an efficiency of 20 %. So these materials are widely explored across the world. Here we tried to synthesize  $\text{MAPbI}_3$  single crystals by Inverse Temperature Crystallization. is of very high importance in recent fields of study.  $\text{MAPbI}_3$  exist in various crystallographic structures. We make use of the techniques such as, structural (XRD), thermal (TGA/DSC), optical (UV-Visible) here in our study to characterize the properties of the grown single crystals. In this chapter we are dealing with the results of characterisation techniques and scope for future study.

### 3.1- EXPERIMENTAL DETAILS

Precursor solutions of different concentrations are produced by blending certain quantity of synthesized MAI and  $\text{PbI}_2$  in gamma- Butyrolactone (GBL).

- Molecular weight of MAI = 158.9695 g/mol

Desired final volume of MAI solution = 5 ml

Molarity = 1.23 M

Mass of Methylamine iodide = 2.8352 g

- Molecular weight of  $\text{PbI}_2$  = 461.01 g/mol

Desired final volume of  $\text{PbI}_2$  = 5 ml

Molarity = 1.23 M

Mass of Lead iodide = 0.9776 g



### 3.2 – Powder X-Ray Diffraction Analysis

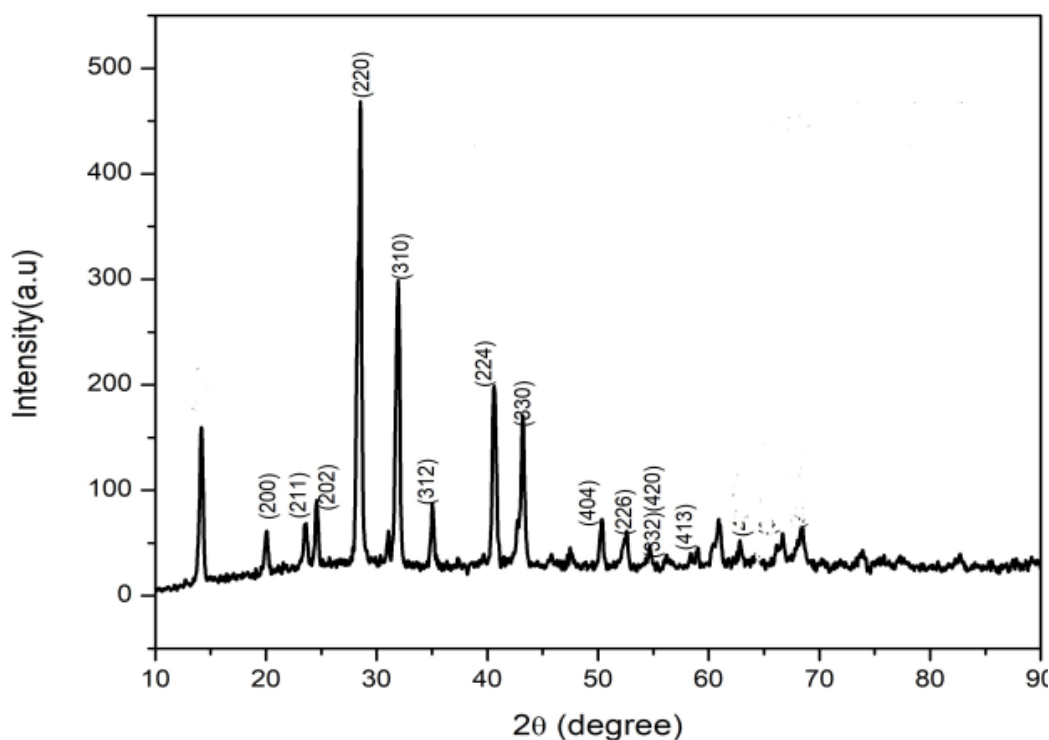


Figure 3.1- Powder XRD of MAPbI<sub>3</sub>

Powder X-ray diffraction measurements were performed on the ground MAPbI<sub>3</sub> single crystal, to further assert the single crystalline nature and structure of the synthesized single crystal of MAPbI<sub>3</sub>. XRD data so collected are compared with ICSD data (ICSD collection code: 238610) [31] (Figure 3.1). A set of preferred orientations[32] corresponding to the planes (110), (220), (310), (224), and (330) were observed at  $2\theta$  values, 14.080, 28.440, 31.850, 40.580 and 43.190 of the MAPbI<sub>3</sub> tetragonal structure, respectively. Minor peaks are also present at  $2\theta$  values of 19.920, 23.540, 24.52, 340.940, 50.220 and 52.540 and are assigned to the planes (112), (211), (202), (204), (404), and (336) respectively. This had confirmed that the grown product is MAPbI<sub>3</sub> single crystal having high material and phase purity. Further, no MAI and PbI<sub>2</sub> characteristic peaks are found to be present in the XRD data, indicating the effectiveness of the washing of the grown crystal with isopropanol and diethyl ether to remove the lead iodide impurity.

### 3.3- UV visible Absorption Spectrum Analysis

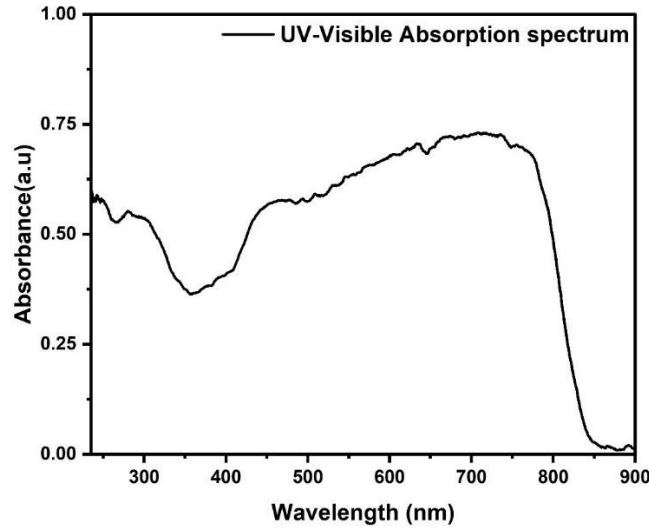


Figure 3.2 - UV-Visible Absorption Spectrum of MAPbI<sub>3</sub>

The UV-Visible absorption spectra of single crystal powder were taken in 200-900 nm range using Avaspec 2048 spectrophotometer equipped with halogen and deuterium lamps. Measurements were carried out at room temperature. Figure 3.2 shows the absorption spectrum of MAPbI<sub>3</sub> single crystals taken in reflection mode. Single crystal possesses excellent light harvesting ability in the visible range till 800 nm. So, they can be used as light harvesting material in solar cells. There is a sudden drop in the absorption after 800nm indicating that the material possesses sharp absorption edge. Absorption edge of polycrystalline counterpart is around 790 nm, the red shift [33] in the upper limit of absorption point towards the effectiveness of using single crystals as light harvesting materials in solar cells. Figure 3.3 shows the Tauc plot for obtaining the bandgap of the material. By using the Tauc plot method, the  $E_g$  is determined through a linear extrapolation of the observed trend in the spectral dependence of  $(\alpha h\nu)^2$  which intercepts the abscissa axis giving by the photon energies  $h\nu$  [34]. By extrapolating the straight-line portion of the curve to the energy axis direct band gap( $E_g$ ) is obtained as 2.94 eV. The mathematical expression governing bandgap calculation is given by

$$(\alpha h\nu)^{(1/\gamma)} = B(h\nu - E_g) \quad (9)$$

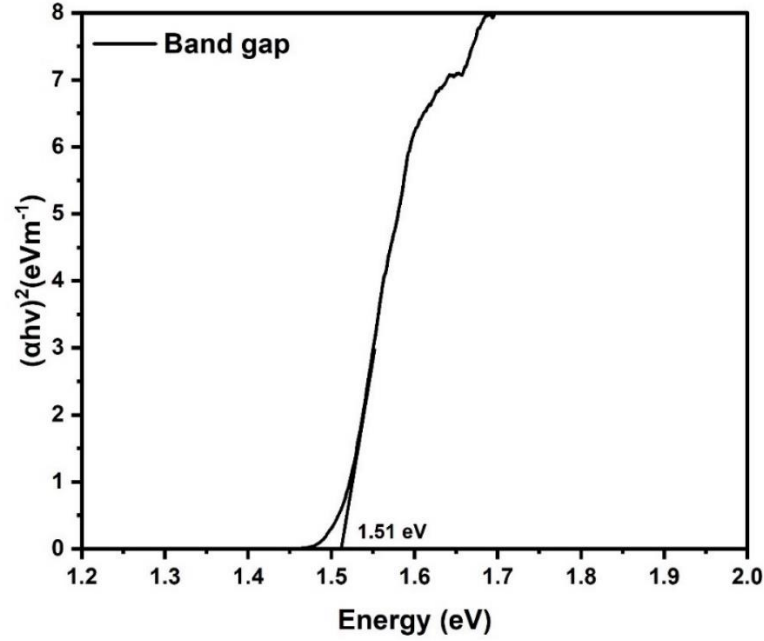


Figure 3.3- Band gap of MAPbI<sub>3</sub>

where  $h$  is the Planck constant,  $\nu$  is the photon's frequency,  $E_g$  is the band gap energy, and  $B$  is a constant. Also, the energy dependent absorption coefficient,

$$\alpha = 2.303 * \left(\frac{A}{d}\right) \quad (10)$$

where  $A$  is the absorbance and  $d$  are the internal width of the cuvette for liquid or thickness in case of film. For direct band gap, the value of  $\gamma$  is  $\frac{1}{2}$  and for indirect, the value is 2.

Band gap is a fundamental quantity that predicts the usefulness of the material in photovoltaic and energy applications. Usually, devices with  $E_g \sim 1.3$  eV[35] are used as acceptor material in solar cells according to Schottky Queisser limit. Bandgap of this material comes the category of semiconducting materials.

### 3.4- Thermogravimetric Analysis

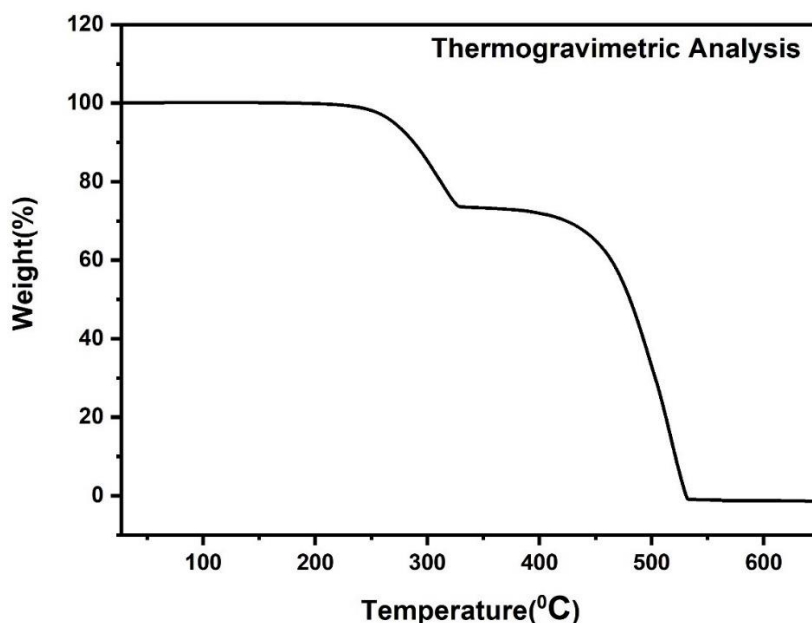


Figure 3.4- Thermogravimetric Analysis of MAPbI<sub>3</sub>

Thermogravimetric Analysis is a technique used for analysing thermal stability and thermal behaviour of the material. The measurement is carried out under nitrogen atmosphere from room temperature to 600°C. The thermogram of powdered MAPbI<sub>3</sub> (Figure 3.4) shows no indication of chemical decomposition or physical changes up to 270°C, and then it undergoes sequential mass loss of 20% and 4%, which may be attributed to the losses due to hydroiodic acid and MA component[33] respectively. The loss of hydroiodic acid and MAI component occurs at 380°C and 450°C respectively. This sequential decomposition indicates that methylammonium (MA) group is bound to perovskite matrix more tightly than hydroiodic acid, as there is no indication of MAI decomposing into HI and MA in the thermogram of MAI. Thus, the TGA analysis points toward the thermal stability of the synthesized MAPbI<sub>3</sub> single crystal.

### 3.5- Differential Scanning Calorimetry

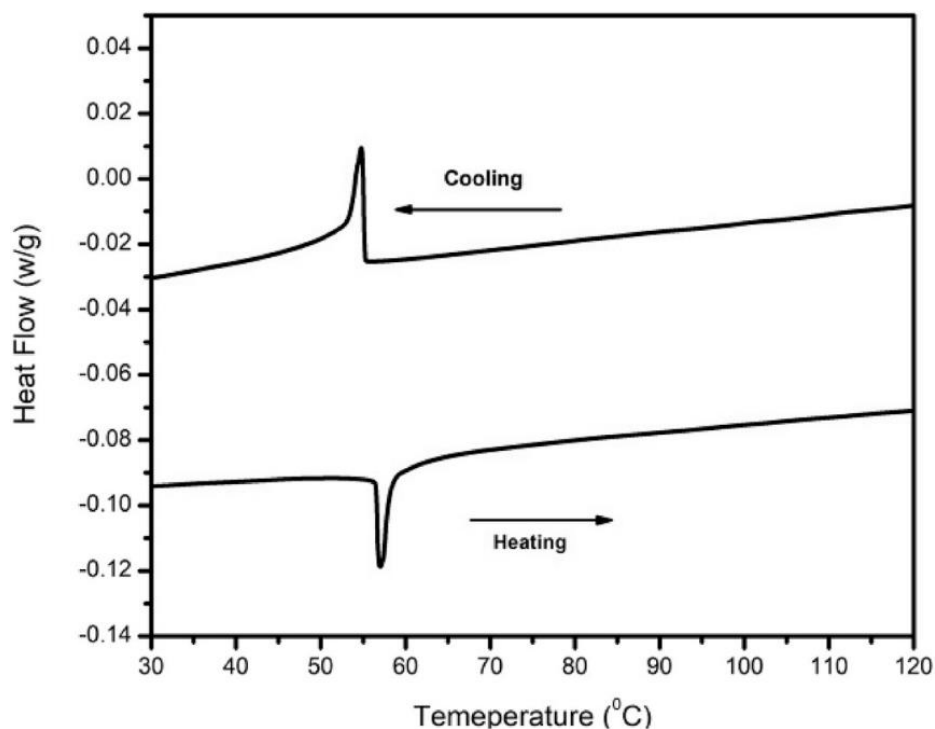


Figure 3.5- Differential Scanning Calorimetry of MAPbI<sub>3</sub>

Differential Scanning Calorimetry (DSC) of the powdered single crystals were taken by heating the DSC pan from -50 °C to 250 °C and cooling back at 10K/min (Figure 3.5). The heating and cooling thermograms show peaks at 57.04 °C and 54.9 °C respectively. This asymmetry of DSC peaks may be arising from [36]the presence of a transient intermediate phase change [36][37]from tetragonal to cubic that takes place in the CH<sub>3</sub>NH<sub>3</sub>PbI<sub>3</sub>. The transition temperatures for this phase change in heating and cooling curve are seen to be different as mentioned above.

### **3.6 – CONCLUSION**

A simple and room temperature MAPbI<sub>3</sub> hybrid perovskite crystal growth process in open atmosphere is developed and high-quality perovskite single crystal has been successfully grown by Inverse temperature crystallization method by optimizing the concentration and temperature of the growth solution. Structural purity of the material was confirmed by powder XRD. DSC and TGA thermograms were used to analyse the thermal behaviour and stability of material.

### **3.7 SCOPE FOR FUTURE STUDY**

Methylammonium Lead Iodide perovskite has been of great concern in recent fields of study. The required single perovskite crystal is made using inverse temperature crystallization method. The interdependence of the structure and property in single crystalline perovskite films is yet to be established to enrich the high-speed photon detection applications. The lower bandgap, larger exciton concentration with reduced recombination, and more effective carrier are difficulties in device applications. gadgets used in industrial settings. To advance this technique, it is necessary to have synthesis control over the orientation and thickness of large-area single-crystal films, pertaining to their incorporation into the photovoltaic devices. To produce Pb-free, all-inorganic perovskites that can pave the way for ambiently stable devices, strategies must be established, and difficulties must be overcome to replace the unstable MA cation and hazardous Pb. Due to their structural relaxations and improved PL intensities, thin 2D perovskite single crystals may be optimal. The use of quasi 2D and hybrid 2D/3D perovskites with Lewis's base surface modifications are attractive candidates for device construction and control. The 2D/3D mixed perovskite single crystals can be used to make more stable single-junction and multi-junction devices by applying the potential improvements. MAPbBr<sub>3</sub> and MAPbI<sub>3</sub> are the organic-inorganic hybrid perovskites that are commonly used for single crystals. Implementation of high-quality perovskite single crystals in applications like LEDs, PDs, and solar cells not only improves the performance of these devices, but also simplifies their structure and facilitates fabrication by several methods. So, in addition to careful optimization of crystal quality improvement, the development of rational surface passivation techniques is needed the most.

## **REFERENCE**

- [1] Eman Assirey Taibah University, “Ideal Cubic Perovskite Structure”.
- [2] E. A. R. Assirey, “Perovskite synthesis, properties and their related biochemical and industrial application,” *Saudi Pharmaceutical Journal*, vol. 27, no. 6. Elsevier B.V., pp. 817–829, Sep. 01, 2019. doi: 10.1016/j.jsps.2019.05.003.
- [3] “Perovskite Crystal.” <https://en.wikipedia.org//>
- [4] “Lev Perovski.” [https://www.wikiwand.com/en/Lev\\_Perovski](https://www.wikiwand.com/en/Lev_Perovski)
- [5] S. C. Wathage, Z. Song, A. B. Phillips, and M. J. Heben, “Evolution of perovskite solar cells,” in *Perovskite Photovoltaics: Basic to Advanced Concepts and Implementation*, Elsevier, 2018, pp. 43–88. doi: 10.1016/B978-0-12-812915-9.00003-4.
- [6] E. A. R. Assirey, “Perovskite synthesis, properties and their related biochemical and industrial application,” *Saudi Pharmaceutical Journal*, vol. 27, no. 6. Elsevier B.V., pp. 817–829, Sep. 01, 2019. doi: 10.1016/j.jsps.2019.05.003.
- [7] “Classification of Perovskites.” doi: [10.1016/j.jsps.2019.05.003](https://doi.org/10.1016/j.jsps.2019.05.003)
- [8] N. F. Atta, A. Galal, and E. H. El-Ads, “Perovskite Nanomaterials – Synthesis, Characterization, and Applications,” in *Perovskite Materials - Synthesis, Characterisation, Properties, and Applications*, InTech, 2016. doi: 10.5772/61280.
- [9] L. Chouhan, S. Ghimire, C. Subrahmanyam, T. Miyasaka, and V. Biju, “Synthesis, optoelectronic properties and applications of halide perovskites,” *Chemical Society Reviews*, vol. 49, no. 10. Royal Society of Chemistry, pp. 2869–2885, May 21, 2020. doi: 10.1039/c9cs00848a.
- [10] S. S. Rong, M. B. Faheem, and Y. B. Li, “Perovskite single crystals: Synthesis, properties, and applications,” *Journal of Electronic Science and Technology*, vol. 19, no. 2, pp. 1–18, 2021, doi: 10.1016/J.JNLEST.2021.100081.

- [11] R. Gupta *et al.*, “Room temperature synthesis of perovskite (MAPbI<sub>3</sub>) single crystal by anti-solvent assisted inverse temperature crystallization method,” *J Cryst Growth*, vol. 537, May 2020, doi: 10.1016/j.jcrysgro.2020.125598.
- [12] “single perovskite crystal picture.” <https://doi.org/10.1016/j.jnlest.2021.100081>
- [13] M. T. Ha, L. van Lich, Y. J. Shin, S. Y. Bae, M. H. Lee, and S. M. Jeong, “Improvement of SiC crystal growth rate and uniformity via top-seeded solution growth under external static magnetic field: A numerical investigation,” *Materials*, vol. 13, no. 3, Feb. 2020, doi: 10.3390/ma13030651.
- [14] H. Shen, R. Nan, Z. Jian, and X. Li, “Defect step controlled growth of perovskite MAPbBr<sub>3</sub> single crystal,” *J Mater Sci*, vol. 54, no. 17, pp. 11596–11603, Sep. 2019, doi: 10.1007/s10853-019-03710-6.
- [15] S. Adjokatse, H. H. Fang, and M. A. Loi, “Broadly tunable metal halide perovskites for solid-state light-emission applications,” *Materials Today*, vol. 20, no. 8. Elsevier B.V., pp. 413–424, Oct. 01, 2017. doi: 10.1016/j.mattod.2017.03.021.
- [16] “photodetector.” <https://www.sciencedirect.com>
- [17] R. Surabhi, K. Bhat, A. Batra, A. Chilvery, and M. Aggarwal, “Synthesis, Purification, Crystal Growth and Characterization of Lead Iodide (PbI<sub>2</sub>) Purified by a Low-Temperature Technique,” *Adv Sci Eng Med*, vol. 6, no. 12, pp. 1269–1273, Jan. 2015, doi: 10.1166/ase.2014.1637.
- [18] “methylammonium iodide.” <https://www.sigmaaldrich.com/>
- [19] “X-Ray Diffraction.” <https://www.sciencedirect.com>
- [20] L. S. U. C. M. C. E. M. U. Barbara L Dutrow, “Powder XRD instrumentation.”
- [21] “Powder XRD.” <https://pubmed.ncbi.nlm.nih.gov/>
- [22] P. Justin Tom, “UV Visible spectroscopy.”



- [23] John P. Rafferty, “Beer’s law.”
- [24] “UV visible.” <https://microbenotes.com/uv-spectroscopy>
- [25] J. Gomes, J. Batra, V. R. Chopda, P. Kathiresan, and A. S. Rathore, “Monitoring and control of bioethanol production from lignocellulosic biomass,” in *Waste Biorefinery: Potential and Perspectives*, Elsevier, 2018, pp. 727–749. doi: 10.1016/B978-0-444-63992-9.00025-2.
- [26] W. Li, X. Y. Tan, Y. M. Park, D. C. Shin, D. W. Kim, and T. G. Kim, “Improved Thermal Resistance and Electrical Conductivity of a Boron-Doped DLC Film Using RF-PECVD,” *Front Mater*, vol. 7, Jul. 2020, doi: 10.3389/fmats.2020.00201.
- [27] “DSC.” <https://www.intertek.com/analysis/dsc>
- [28] HITACHI, “DSC Equipment.”
- [29] K. Kv, A. Sr, Y. Pr, P. Ry, and B. Vu, “Research and Reviews: Journal of Pharmaceutical Analysis Differential Scanning Calorimetry: A Review.”
- [30] P. Gill, T. T. Moghadam, and B. Ranjbar, “Differential Scanning Calorimetry Techniques: Applications in Biology and Nanoscience,” 2010.
- [31] Y. Yamada *et al.*, “Dynamic Optical Properties of  $\text{CH}_3\text{NH}_3\text{PbI}_3$  Single Crystals As Revealed by One- and Two-Photon Excited Photoluminescence Measurements,” *J Am Chem Soc*, vol. 137, no. 33, pp. 10456–10459, 2015, doi: 10.1021/jacs.5b04503.
- [32] P. Fan *et al.*, “High-performance perovskite  $\text{CH}_3\text{NH}_3\text{PbI}_3$  thin films for solar cells prepared by single-source physical vapour deposition,” *Sci Rep*, vol. 6, no. 1, p. 29910, 2016, doi: 10.1038/srep29910.
- [33] P. M and P. Predeep, “Hybrid perovskite single crystal with extended absorption edge and environmental stability: Towards a simple and easy synthesis procedure,” *Mater Chem Phys*, vol. 239, no. April 2019, p. 122084, 2020, doi: 10.1016/j.matchemphys.2019.122084.

- [34] R. E. Aderne *et al.*, “On the energy gap determination of organic optoelectronic materials: The case of porphyrin derivatives,” *Mater Adv*, vol. 3, no. 3, pp. 1791–1803, 2022, doi: 10.1039/d1ma00652e.
- [35] S. Kim *et al.*, “A band-gap database for semiconducting inorganic materials calculated with hybrid functional,” *Sci Data*, vol. 7, no. 1, pp. 1–6, 2020, doi: 10.1038/s41597-020-00723-8.
- [36] T. Baikie *et al.*, “Synthesis and crystal chemistry of the hybrid perovskite (CH<sub>3</sub>NH<sub>3</sub>)PbI<sub>3</sub> for solid-state sensitised solar cell applications,” *J Mater Chem A Mater*, vol. 1, no. 18, p. 5628, 2013, doi: 10.1039/c3ta10518k.
- [37] A. Dualeh, P. Gao, S. Il Seok, M. K. Nazeeruddin, and M. Grätzel, “Thermal behavior of methylammonium lead-trihalide perovskite photovoltaic light harvesters,” *Chemistry of Materials*, vol. 26, no. 21, pp. 6160–6164, 2014, doi: 10.1021/cm502468k.